J. Membrane Biol. 115, 129–143 (1990)

The Journal of
Membrane Biology

Transport of Potassium in *Chara australis:* II. Kinetics of a Symport with Sodium

S.R. McCulloch, M.J. Beilby, and N.A. Walker
Biophysics Laboratory, School of Biological Sciences, University of Sydney, New South Wales, 2006, Australia

Summary. An electrogenic K^+-Na^+ symport with a high affinity for K^+ has been found in *Chara* (Smith & Walker, 1989). Under voltage-clamp conditions, the symport shows up as a change in membrane current upon adding either K^+ or Na^+ to the bathing medium in the presence of the other. Estimation of kinetic parameters for this transport has been difficult when using intact cells, since K^+-Na^+ current changes show a rapid falling off with time at K^+ concentrations above 50 μM. Cytoplasm-enriched cell fragments are used to overcome this difficulty, since they do not show the rapid falling off of current change seen with intact cells. Current-voltage curves for the membrane in the absence or presence of either K^+ or Na^+ are obtained, yielding difference current-voltage curves which isolate the symport currents from other transport processes. The kinetic parameters describing this transport are found to be voltage dependent, with K_m for K^+ ranging from 30 down to 2 μM as membrane potential varies from -140 to -400 mV, and K_m for Na^+ ranging between 470 and 700 μM over a membrane potential range of -140 to -310 mV.

Two different models for this transport system have been investigated. One of these involves the simultaneous transport of both the driver and substrate ions across the membrane, while the other allows for the possibility of the two ions being transported consecutively in two distinct reaction steps. The experimental results are shown to be consistent with either of these cotransport models, but they do suggest that binding of K^+ occurs before that of Na^+, and that movement of charge across the membrane (the voltage-dependent step) occurs when the transport protein has neither K^+ nor Na^+ bound to it.

Key Words electrogenic · sodium-potassium symport · cotransport · charophyte · *I-V* curves · difference *I-V* curves

Introduction

Under normal physiological conditions, the uptake of K^+ by *Chara* can be explained by passive diffusion (Hope & Walker, 1961). Voltage-dependent K^+ current channels are now considered to be the mechanism by which this process occurs (e.g., Kitasato, 1973; Walker, 1980; Keifer & Lucas, 1982; Smith, 1984; Beilby, 1986*a,b*; Smith, Smith & Walker, 1987). However, it has been noted (Smith & Walker, 1989) that *Chara* may grow under some conditions in which the concentration of K^+ is so low that the explanation of K^+ uptake by passive diffusion is no longer possible; instead uphill inward transport would be necessary in order to maintain the cytoplasmic concentration of K^+ at around 100 mM. Similar situations for other plants and fungi have been reviewed by Rodriguez-Navarro, Blatt and Slayman (1986). Known uphill transport mechanisms include a K^+-H^+ symport in *Streptococcus faecalis* (Bakker & Harold, 1980), and also in *Neurospora crassa* (Rodriguez-Navarro et al., 1986; Blatt, Rodriguez-Navarro & Slayman, 1987). In the latter case it was found necessary to starve the cells of K^+ in order to activate the transport. This elicited a high-affinity potassium uptake system, with a stoichiometry of one K^+ entering for each H^+ ion. Detailed kinetics of this transport system were modelled by Blatt et al. (1987).

Smith and Walker (1989) observed that after *Chara* internodal cells had been pretreated in K^+-free solutions for some time, low concentrations of K^+ produced large fluxes of K^+ (measured either by current changes or by radioactive tracers) across the cell membrane. They also found that Na^+, rather than H^+, was necessary for this transport process to occur. Conversely, current changes associated with Na^+ were only observed in the presence of K^+. Radioactive tracer flux experiments indicated that the most likely stoichiometry for this symport was $1K^+ : 1Na^+$.

Transport rate measurements at cell resting potentials were fitted to the Michaelis-Menten equation in order to obtain estimates for the kinetic parameters of this symport (Smith & Walker, 1989). These authors found that as the external concentration of K^+ ($[K^+]_o$) was raised, the current change appeared to saturate with a K_m of approximately 30 μM. They also noted that this measurement was difficult, due to a rapid falling off with time of current changes produced by the higher K^+ concentrations. Similarly, when $[Na^+]_o$ was varied while

$[K^+]_o$ remained constant, saturating kinetics were observed with a K_m of about 470 μM.

The findings of Smith and Walker (1989) demonstrated that *Chara* has an electrogenic transporter with a relatively high affinity (low K_m) for K^+. In this present study, we begin a detailed investigation into the kinetics of this K^+-Na^+ symport using both intact cells and cytoplasm-enriched cell fragments.

Materials and Methods

Plant Material

The experimental material was *Chara australis* R. Br. (= *C. corallina* em. R.D.W). Expression of the K^+-Na^+ transport system usually required the pretreatment or "starving" of cells in a K^+-free medium for periods of 2–4 weeks. This solution contained 0.1 mM $CaCl_2$ and 1 mM NaCl. Cells from one culture showed currents without being K^+ starved (although they had grown in a reasonable K^+ concentration in the culture medium), suggesting that there may also be conditions other than K^+ starvation that will cause the transport protein to be expressed.

Internodal cells, with their nodes still intact, were removed from the whole plant and placed in the K^+-free solution. This solution was changed once every 3–5 days. Batches of cells were kept in large petri dishes under a fluorescent light source, switched on for 12 hr per day. After 2 to 3 weeks, many of the internodes were observed to have sprouted small shoots, and occasionally rhizoids, from their nodes.

Cytoplasm-Enriched Cell Fragments

The cytoplasmic layer in intact cells is only about 10 μm thick, so that approximately 95% of the cell volume is occupied by vacuole (Peebles, Mercer & Chambers, 1964; Bostrom & Walker, 1975; Sakano & Tazawa, 1984). In this study, membrane current changes showed a rapid falling off with time when using intact cells, making it difficult to obtain accurate transport rate measurements. It has been suggested that this effect is most likely to arise from changes in cytoplasmic Na^+ during the course of an experiment (Smith & Walker, 1989).

Cytoplasm-enriched cell fragments, however, can be treated for electrical studies simply as cytoplasm enclosed by a plasmalemma and cell wall (Beilby & Blatt, 1986), thus eliminating many of the complications caused by the presence of a vacuole and tonoplast. Their behavior is otherwise analogous to that of intact cells under a wide range of conditions, and they have also been shown to display most of the electrical characteristics of intact cells (Beilby & Blatt, 1986; Beilby & Shepherd, 1989). One exception to this is that the diminished excitation of such fragments allows them to be voltage clamped over a wide range of potentials without deleterious effect (Beilby & Blatt, 1986). It was hoped that in this study, the large cytoplasmic volume of cytoplasm-enriched fragments (compared with intact cells) would cause influxes of K^+ and Na^+ to have only a small effect on the total cytoplasmic concentrations of these ions.

The procedure used to obtain cytoplasm-enriched fragments was similar to that described previously by Hirono and Mitsui (1981) for obtaining cell fragments from *Nitella*. Pretreated internode cells of *Chara* were centrifuged at about 1000 rpm in a Clements GS200 benchtop centrifuge for 30 min, during which time a cytoplasmic plug would form at the end of the cell. A thread (silk or polyester) was then used to tie off this plug from the remainder of the cell, which could then be removed. The reappearance of cytoplasmic streaming (usually about 30 min after preparation) and a "tight" (regular) arrangement of chloroplasts were used as the criteria for selecting experimentally viable cell fragments after this procedure.

Electrical Measurements

For measurement of membrane currents from intact cells, voltage-clamping was achieved by means of external electrodes. The apparatus and method for this procedure has been described previously (Smith & Walker, 1989). Essentially this method clamps the membrane as its resting potential, but this potential is not measured. For electrical measurements on cytoplasm-enriched cell fragments, inserted microelectrodes were used. Microelectrodes were pulled on a Narishige pipette puller using "Kwik-fil" glass capillary tubes containing an inner filament that facilitated the filling of these electrodes with 3 M KCl. Connections between the microelectrode filling solutions and the circuitry were by means of chloride-coated silver wires. A 25-μm Pt/Ir wire electrode inserted longitudinally into the cell fragment enabled the whole membrane to be space clamped. The voltage-clamp apparatus and software used in experiments on cytoplasm-enriched fragments has been described previously by Beilby and Beilby (1983). *I-V* curves were obtained by measuring the changes in membrane currents, while the membrane potential was clamped to a bipolar staircase at a pulse width of 60 msec and pulse separation 320 msec. Current measurements were obtained during the last few milliseconds of each pulse, by which time a steady-state current had been reached. Under such conditions, and at the K^+ concentrations used in these experiments, the contribution to the *I-V* curves from voltage-dependent K^+ channels is negligible (Smith, 1984; Beilby 1986*a*,*b*).

Chemicals and Solutions

All chemicals used in experiments were A.R. grade. Solutions were made using deionized water from a Millipore Milli-Q filtration system which produced water of resistivity 18 MΩ cm. These were made fresh each day from stock solutions to avoid the possibility of contamination, either from ammonium ions (Walker, Beilby & Smith, 1979), which might accumulate over a period of time, or the presence of micro-organisms which may alter the low ionic concentrations or pH of the solutions. Both effects could significantly alter results of these experiments if unchecked, since very low concentrations of K^+ typically give rise to currents of similar magnitude to those which may be produced by either of these phenomena.

Solutions used were unbuffered, with a pH of about 5.6. K^+ and Na^+ were added as either Cl^- or SO_4^{2-} solutions; all solutions contained 0.1 mM $CaCl_2$.

Estimation of Kinetic Parameters

The Briggs-Hill-Whittingham equation (Hill & Whittingham, 1957) was fitted to data for current changes measured upon

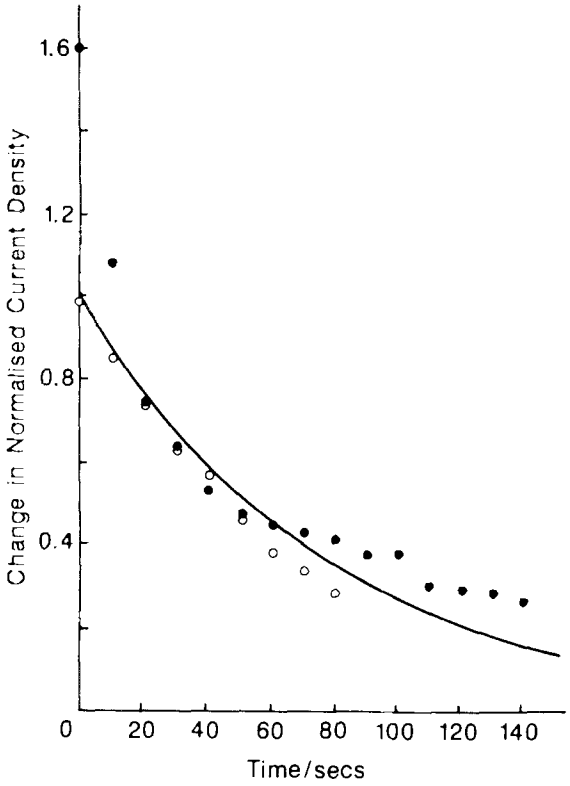

Fig. 1. Time course of changes in membrane current I in cells clamped at their resting potential, produced by exposure to 100 μM K^+ in a background solution of 1 mM NaCl and 0.1 mM $CaCl_2$. Filled and open symbols distinguish between results from two different intact cells, which taken separately can be fitted roughly by exponentially decreasing functions, with half times of 44 and 65 sec. (Current normalized to $I_o \approx 10.6$ mA m^{-2}, the initial value of the exponential function)

changing $[K^+]_o$, to account for the presence of unstirred layers adjacent to the cell membrane. This was achieved using the "robust" method of parameter estimation described by Press et al. (1987). In order to perform the required minimization, the Fortran subroutine "Amoeba" (Press et al., 1987) was rewritten in Microsoft Basic and run on a Compaq Portable II computer. For results obtained from variation of $[Na^+]_o$, where unstirred layers were not significant, the data was fitted using the same routine, but with P_u, the unstirred layer permeability fixed and very large. In this case, the Briggs-Hill-Whittingham equation reduces to the simpler Michaelis-Menten equation.

Results

Currents Induced in Intact Cells by K^+

Current changes induced by exposing intact cells to K^+ were observed to fall off rapidly during the period of exposure. Indeed, the current response depended somewhat on any previous exposure to K^+.

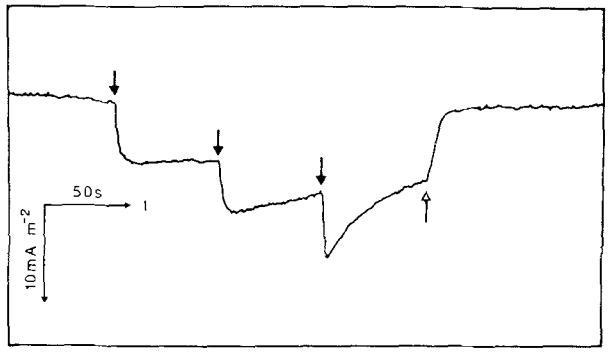

Fig. 2. Effect of varying $[K^+]_o$ on the rate of current turnoff, measured on an intact cell under voltage-clamp conditions. Background solutions were 1 mM NaCl and 0.1 mM $CaCl_2$. Solid (down) arrows represent solution changes to 4, 12 and 100 μM K^+ in the outside medium, respectively; open (up) arrow indicates return to background solution

Such a dependence on previous exposure to a substrate has been observed for amine transport (Walker et al., 1979). In this case it was found that the turnoff rate could be represented approximately by a decreasing exponential function. An analogous treatment of results for K^+-Na^+ symport currents from two cells is shown in Fig. 1, demonstrating that the current induced by 100 μM K^+ may also be roughly fitted by an exponentially decreasing function, with half times of 44 and 65 sec for each cell, respectively.

The rate of turning off was also found to depend on the external concentration of K^+, as well as on the magnitude of the membrane current. This effect is illustrated in Fig. 2, which shows that the membrane current decays much more rapidly upon exposure to 100 μM K^+ than upon exposure to 4 or 12 μM K^+, in spite of the similarity in the sizes of the currents.

Because of this rapid turnoff, it was difficult to obtain reliable current measurements from a large number of exposures to different concentrations of K^+. An attempt was made to minimize the effects of current turnoff by estimating the kinetic parameters from data on cells subjected to as few successive exposures to K^+ as possible. Using this approach, the parameters K_m and V_{max} were obtained for 49 cells. The results showed a wide scatter of values: K_m and V_{max} had medians of 7 μM and 7 mA m^{-2} with 95% confidence intervals of 5 to 10 μM and 5 to 11 mA m^{-2}, respectively. There was a correlation between K_m and V_{max} which was significant at the 99% level. This association of high measured K_m with high values of V_{max} suggested to us that the apparent K_m was being increased by an unstirred layer effect (*see below*).

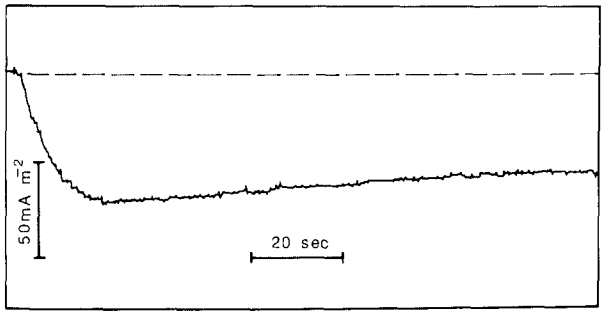

Fig. 3. Time course of current measured from a cytoplasm-enriched voltage-clamped cell fragment upon exposure to 100 μM K^+. Half time for the current turnoff is of the order of 10 min (*cf.* Fig. 2) where membrane current induced by 100 μM K^+ has a half time of about 10 sec. Background solution is 1 mM NaCl and 0.1 mM $CaCl_2$

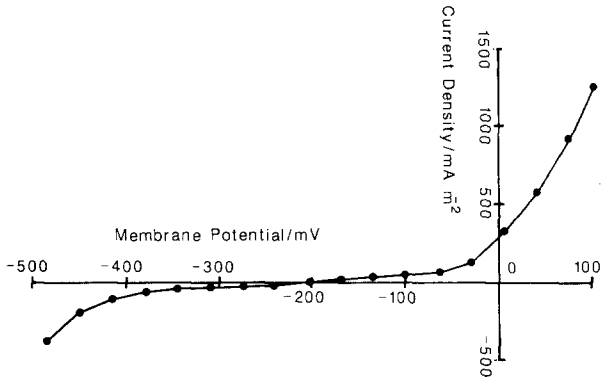

Fig. 4. Typical *I-V* curve from a K^+-starved cell fragment, bathed in 1 mM NaCl and 0.1 mM $CaCl_2$. Beyond about −400 mV, the onset of punchthrough becomes dominant, while at potentials positive to −50 mV the rectifier current predominates the *I-V* curve

Measurements from Cell Fragments

An alternative approach to reducing current turnoff is using cytoplasm-enriched cell fragments instead of whole cells as experimental material. Figure 3 shows current *vs.* time recorded for the exposure of a K^+-starved cell fragment to 100 μM K^+. Comparison with intact cell results shows a marked reduction in the rate of turnoff in the cell fragment, as expected. Whereas the current induced by 100 μM K^+ in the whole cell fell to about half its initial value in about 10–40 sec (Figs. 1 and 2), the equivalent current in a cell fragment had a half time of the order of 10 min.

General Characteristics of the I-V Curves

While the apparatus enabled a large voltage range to be scanned in a short time interval, the actual range over which the cell fragment could be clamped was limited by several factors: first, at large negative (hyperpolarizing) potentials, a large increase in membrane conductance occurs (Coster, 1965), which involves a large Cl^- outflow (Coster & Hope, 1968; Coleman, 1986; Tyerman, Findlay & Paterson, 1986*a*,*b*). At depolarized membrane potentials, a very large outward current occurs, sometimes referred to as an outward rectifying current (Felle, 1981). Both phenomena involve large currents through the plasmalemma, which may alter some properties of the cell.

For this reason *I-V* curves were limited to within these voltage extremes, allowing typical voltage ranges of about −400 to 0 mV. For each cell, the particular range was determined from preliminary *I-V* runs. Figure 4 shows an *I-V* curve from a K^+-starved cell for which the accessible range of membrane potentials was particularly large. In this figure, the onset of punchthrough and of rectification may be seen in the voltage extremes.

Apparent Current-Voltage Characteristics for the K^+-Na^+ Symport

For each cell fragment, a series of *I-V* curves was obtained at different K^+ or Na^+ concentrations. Figure 5 shows examples of such *I-V* curves, (*a*) during brief exposures to various $[K^+]_o$ at constant $[Na^+]_o$ and (b) during brief exposures to various $[Na^+]_o$ at constant $[K^+]_o$. In each case, the depolarization (shift of the intercept of the curve on the voltage axis) varied with ion concentration. It is not easy to make meaningful comparisons of "resting potential" between Fig. 5*a* and *b*.

Difference Current-Voltage Curves

The *I-V* curves as described above are the result (or sum) of all transport processes that occur across the plasmalemma under the prevailing experimental conditions. In order to determine the *I-V* characteristics specific to a single transport process, it is necessary to separate the K^+- and Na^+-induced currents from other transport processes. This is achieved by examining the difference current-voltage (*dI-V*) curves. Figure 6*a* and *b* shows the corresponding difference curves obtained from the *I-V* curves of Fig. 5*a* and *b*, respectively, by subtracting the *I-V* curves obtained in the absence of either $[K^+]_o$ and $[Na^+]_o$, from each subsequent curve. These results demonstrate that for this symport process mem-

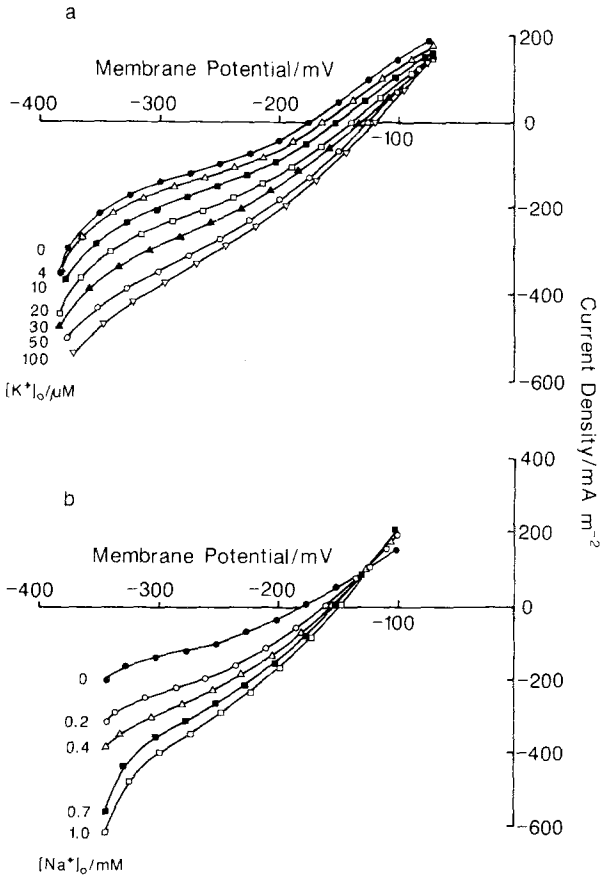

Fig. 5. *I-V* curves for a K^+-starved, cytoplasm-enriched cell fragment in the presence of (*a*) various $[K^+]_o$ in a background of 0.1 mM $CaCl_2$ and 1 mM NaCl, and (*b*) various $[Na^+]_o$ in a background of 0.1 mM $CaCl_2$ and 200 μM KCl

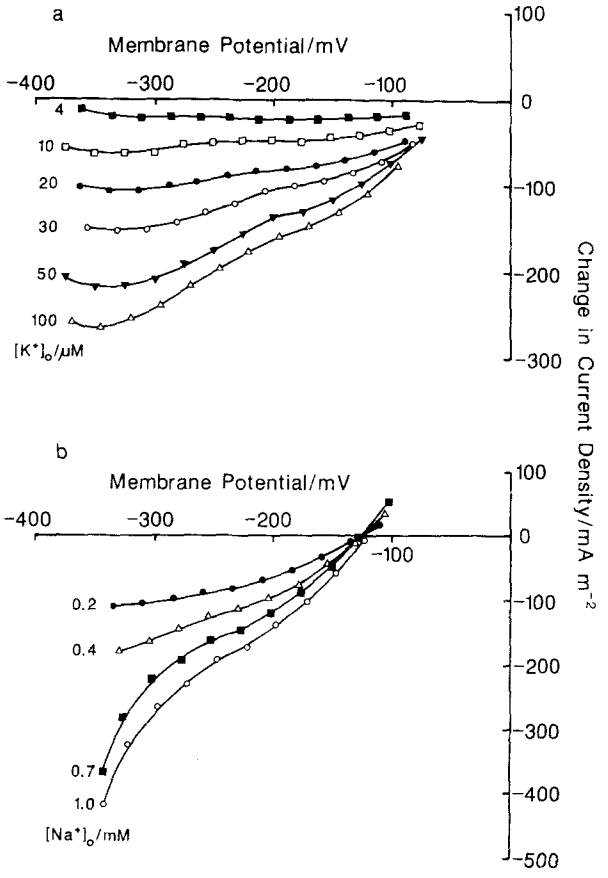

Fig. 6. Difference current-voltage curves obtained from the *I-V* curves of Fig. 5, for (*a*) various $[K^+]_o$, and (*b*) various $[Na^+]_o$

brane potential has a significant effect on the transport. An important point to note, however, is that in many cases the difference curves were observed to cross the voltage axis at more positive potentials (e.g., Fig. 6*b*), contrary to the prediction by Blatt (1986) that *dI-V* curves should always lie below the voltage axis.

The Effect of Membrane Potential on Kinetic Parameters

It can be shown (Blatt, 1986) that, in general, difference currents measured at any one membrane potential will show Michaelian-type kinetics. Thus, for each cell it is possible to obtain a series of current *vs.* concentration curves from the difference curves by measuring the currents each membrane potential sampled. Such curves were obtained for the variation of both $[K^+]_o$ and $[Na^+]_o$.

Figure 7*a* shows the effect of varying $[K^+]_o$ and membrane potential on the symport current. The results were found to be best fitted by the Briggs-Hill-Whittingham equation, in order to allow for the presence of unstirred layers. Clearly the currents are voltage dependent, with the membrane currents increasing at any given concentration of K^+ as membrane potential becomes more negative.

Figure 7*b* shows analogous results to those of Fig. 7*a* for the case when $[Na^+]_o$ is varied. Most results for Na^+ were obtained in the absence of an exchange ion, so that anion concentration also varied to some degree with Na^+. (For experiments involving changes in $[K^+]_o$ in the range 0–200 μM, changes in anion concentration were considered negligible.) In a single experiment choline chloride was added to maintain constant anion concentration as the concentration of Na^+ was varied. Results from this experiment were not significantly different from those obtained when anion concentration was allowed to vary.

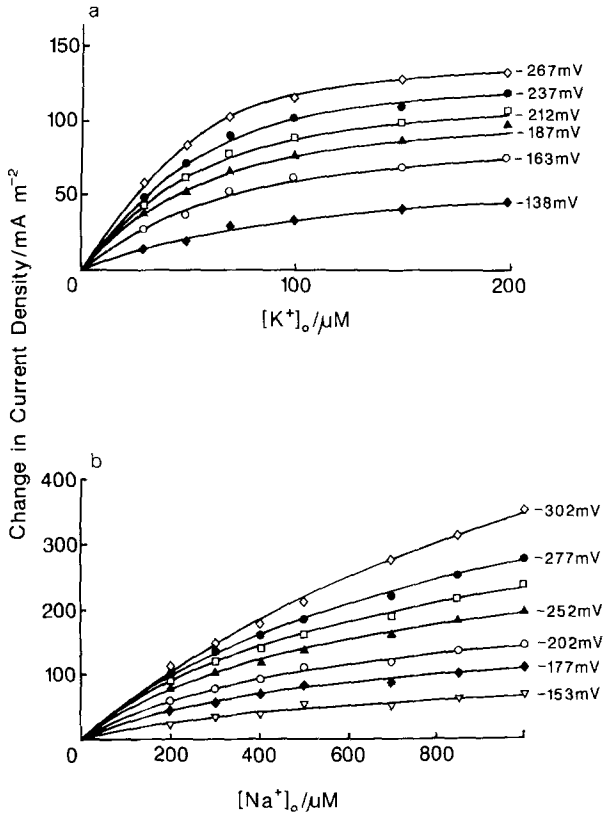

Fig. 7. (*a*) Current *vs.* external K^+ concentration curves for a cytoplasm-enriched cell fragment, showing the effect of changing membrane potential in a cytoplasm-enriched cell fragment. Solid lines represent fits to the Briggs-Hill-Whittingham equation. (*b*) Current *vs.* external Na^+ concentration curves, showing the effect of changing membrane potential in a cytoplasm-enriched cell fragment. Solid lines represent fits to the Briggs-Hill-Whittingham equation with P_u fixed and very large, so that the data is fitted essentially to the Michaelis-Menten equation

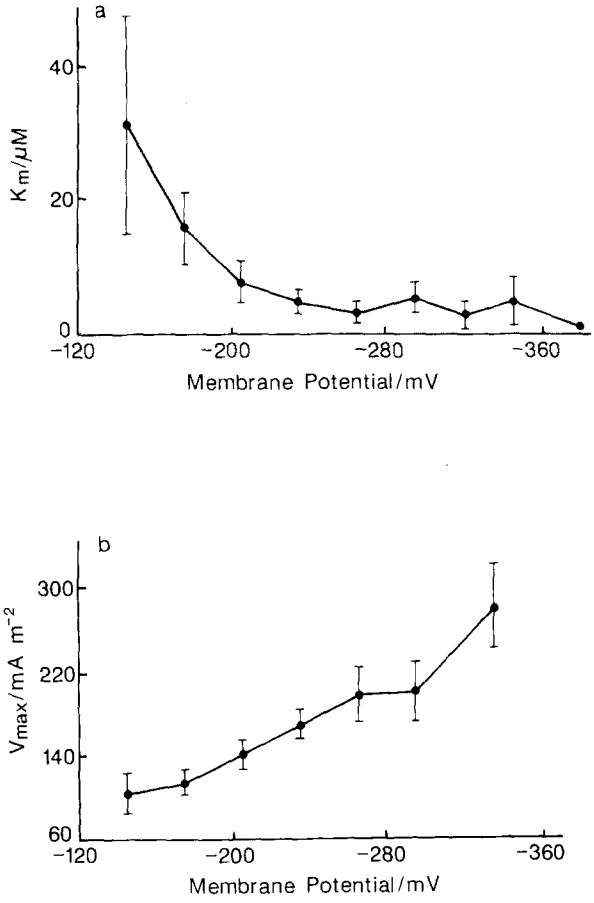

Fig. 8. Variation with membrane potential of the kinetic parameters (*a*) K_m and (*b*) V_{max} for external K^+. Points are mean values ± SEM (obtained from 7 cytoplasm-enriched cell fragments)

Estimates of Unstirred Layer Permeability

Estimates of the unstirred layer permeability P_u varied somewhat between experiments. Typically values were about 5×10^{-5} m sec^{-1}, corresponding to an unstirred layer of water approximately 40 μm thick, but in at least one case a layer as thick as 80 μm was recorded. These results are consistent with estimates of unstirred layer thicknesses in amine transport experiments on *Chara* (Walker et al., 1979), which had a median of 40 μm, but were as high as 150 μm.

Estimates of K_m and V_{max}

A plot showing how the kinetic parameters obtained from such curves vary with membrane potential is illustrated in Fig. 8. From this it can be seen that V_{max} increases as membrane potential becomes more negative. On the other hand, K_m for K^+ shows the opposite dependence, decreasing as membrane potential becomes large and negative. This represents an increase in the apparent affinity of the protein for K^+ as membrane potential becomes more negative. Average values for K_m range from about 30 μM at −130 mV, down to only a few micromolars at large negative potentials. At resting potentials around −200 mV, Fig. 8 shows that the average K_m was about 10 μM. This is consistent with the estimates suggested by results from intact cells, but is somewhat less than the value estimated by Smith and Walker (1989) as 30 μM.

As with results from $[K^+]_o$ variation, $[Na^+]_o$ symport currents were seen to increase as membrane potential becomes more negative. This can be seen in the plot of V_{max} as a function of membrane potential in Fig. 9. This figure also shows that Na^+ is unlike K^+ in that the values of K_m increase with

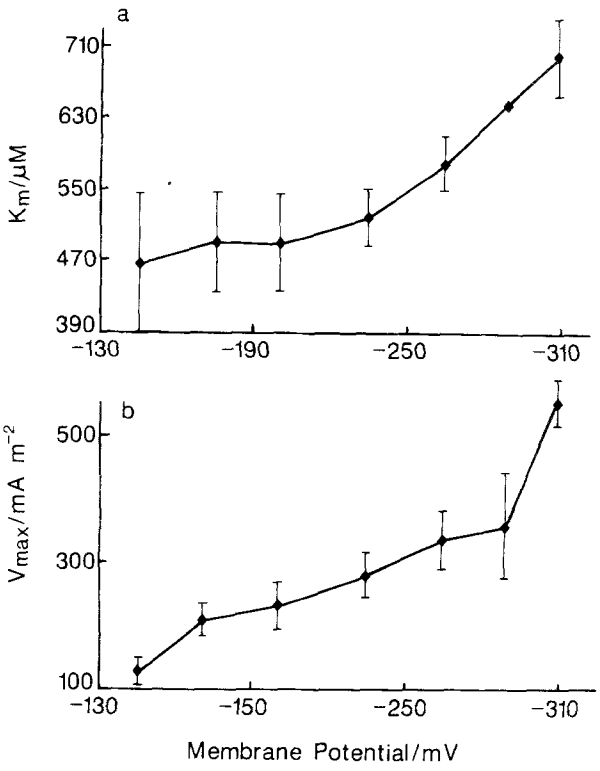

Fig. 9. Variation with membrane potential of the kinetic parameters (*a*) K_m and (*b*) V_{max} for external Na^+. Points are mean values ± SEM (obtained from five cytoplasm-enriched cell fragments)

increasing negative potential. They range from about 470–700 μM as membrane potential varies from −145 to −310 mV. Furthermore, Fig. 9 shows that K_m for Na^+ was about 500 μM at −200 mV, which is consistent with the results of Smith and Walker (1989).

Discussion

The Phenomenon of Current Turnoff

We observed a rapid turnoff of the membrane currents over time. This phenomenon was also noted in the earlier study of the K^+-Na^+ symport by Smith and Walker (1989). Although a similar effect has been observed with amine transport (Walker et al., 1979), the turnoff half times observed in that example were 500 and 900 sec for two separate cells. The much shorter half times of 44 and 65 sec observed for the K^+-Na^+ transport, however, mean that even very brief exposure to higher K^+ concentrations will significantly reduce the cell's response on subsequent exposures to K^+.

A Model for the Turnoff—Product Inhibition

The Michaelis-Menten equation strictly applies only to the measurement of initial transport reaction rates when the complicating effects of product accumulation do not apply. In many cases, as with this K^+-Na^+ symport, it is difficult to achieve steady-state conditions under which the reaction proceeds at a constant rate over an appreciable period of time. In the study of enzyme kinetics it is often possible largely to overcome this problem by the use of the "integrated Michaelis-Menten equation" (*see* Eilam & Stein, 1974; Cornish-Bowden, 1979). Unfortunately, these equations are usually not applicable to conditions under which electrophysiological experiments are carried out.

The phenomenon of turnoff can most simply be understood in terms of an accumulation of transported products, which then inhibit the forward transport reaction. In the case of K^+-Na^+ transport, the likely candidate for this inhibition is Na^+ since, as suggested by Tazawa, Kishimoto and Kikuyama (1974), cytoplasmic Na^+ concentrations ($[Na^+]_c$) may be as low as 3 mM, while $[K^+]_c$ is about 80 mM. Thus as K^+ and Na^+ are transported into the cell $[K^+]_c$ will change relatively little, but $[Na^+]_c$ may increase significantly from its (low) initial value, resulting in inhibition. The effect of this is clearly seen in Fig. 2, which shows how the symport current rapidly changes with time and, in addition, how this effect is much more prominent at higher $[K^+]_o$. This is an important point, since it was frequently observed that the rate of turnoff did not depend only on the size of membrane currents. Because of its low K_m, a low and a high concentration of K^+ can produce currents of similar magnitude, but the rate of turnoff is always greater at the higher K^+ concentration.

A similar result was also observed by Beilby and Walker (1981) for a Cl^--$2H^+$ symport in *Chara*. As with the K^+-Na^+ symport, chloride influx can be stimulated by starving the cells of Cl^-, which elicits a high affinity cotransport system for Cl^- (Sanders, 1980). At higher Cl^- concentrations, porter currents were observed to fall with time, and consistent with this is the fact that the values of V_{max} showed a steady fall during successive determinations. Beilby and Walker (1981) suggested that the controlling factor was indeed $[Cl^-]_c$, although this has not been established.

In order to provide some explanation of this effect for the K^+-Na^+ symport, it is necessary to consider the complete rate equation for the symport of two positive ions into the cell. The expression for the current I through the symport (Blatt, 1986) can be written in the following form:

$$I = \frac{[K^+]_o}{k_1^f \cdot [K^+]_o + K^r \cdot (k_2^f \cdot [K^+]_o + k_1^r) + k^{fr}} \quad (1)$$

where k^f and k^r are constants containing forward and reverse reaction rate constants, respectively, and k^{fr} contains both forward and reverse reaction rate constants. Although $[K^+]_c$ and $[Na^+]_c$ do not appear explicitly in this expression, they are implicit in the value of K^r. Assuming $[K^+]_c$ to remain almost constant, K^r will be a linear expression in $[Na^+]_c$, so that Eq. (1) may be rewritten as

$$I = \frac{[K^+]_o}{k_1 \cdot [K^+]_o + k_2 \cdot [K^+]_o \cdot [Na^+]_c + k_3 \cdot [Na^+]_c + k_4} \quad (2)$$

where distinction between forward and reverse rate constants has been dropped. Although the dependence on $[Na^+]_c$ has been argued somewhat qualitatively here, the result is consistent with the expression for the net current given by Sanders (1986) in which $[K^+]_c$ and $[Na^+]_c$ were considered explicitly throughout.

Because $[Na^+]_c$ appears only in the denominator of this expression, the current I will always tend to decrease with time as $[Na^+]_c$ increases. In addition, the presence of the cross-term $[K^+]_o \cdot [Na^+]_c$ means that the effect will always be greater at higher $[K^+]_o$, and not simply proportional to the size of the current I. This is consistent with the experimental observations described earlier.

Equation (2) further suggests that, according to this model, a reciprocal plot of $1/I$ against $[Na^+]_c$ should yield a straight line for any fixed $[K^+]_o$. Although it was not possible to measure $[Na^+]_c$ directly, the total charge Q, which entered the cell over the course of an exposure to $[K^+]_o$, could be estimated from the area under the trace of current *vs.* time. Since $[Na^+]_c$ should be a linear function of Q (or more correctly $Q/2$ if half the total current is carried by Na^+ and half by K^+), a plot of $1/I$ *versus* Q should also yield a straight line at any fixed $[K^+]_o$. Such a plot was obtained and is shown in Fig. 10.

While this model provides some insight into the possible mechanism for current turnoff, it is unable to quantitatively account for the extremely rapid turnoff seen at high $[K^+]_o$. Thus in Fig. 10 the slope of $1/I$ at 100 μM K^+ is considerably less than would be predicted by this model. It is not clear what may be the cause of this. Nevertheless, this model demonstrates one of the expected effects of increasing $[Na^+]_c$, and it may be useful in interpreting the turning off of chloride porter current.

Presence of Unstirred Layers

There were several unexpected features in the measurements of K_m and V_{max}. The first is that all the values of K_m were lower than the previous estimate of about 30 μM (Smith & Walker, 1989), and the median (7 μM) was much lower. Secondly, the results showed a strong correlation between K_m and V_{max}. This correlation could be produced by the presence of an unstirred layer of solution adjacent to the plasmalemma (Barry & Diamond, 1984). If this unstirred layer is not accounted for, K_m will tend to be overestimated, particularly for cells with a high V_{max}. Hence the most reliable estimates of K_m are likely to be those readings for which V_{max} was small. From the intact cell measurements, it would therefore appear that K_m may be as low as a few micromolars. This was confirmed by the results from cytoplasm-enriched cell fragments, which showed K_m for K^+ to be around 10 μM near normal cell resting potentials. Such a high affinity for K^+ is comparable to that found for a K^+-H^+ symport in *Neurospora,* where values for K_m have been reported to be in the range 1–10 μM (Rodriguez-Navarro et al., 1986). The discrepancy between the previous estimate of K_m (30 μM) and those reported here is probably due to the fact that an effect of unstirred layers was considered unlikely by Smith and Walker (1989) and was not allowed for. Hence the value that they obtained for K_m was an overestimate.

Measuring the Kinetic Parameters

The K^+-Na^+ Symport in Cell Fragments

While it has been shown that cytoplasm-enriched fragments of *Chara* are analogous to intact cells in many ways (Beilby & Blatt, 1986; Beilby & Shepherd, 1989), there remains the question as to whether the behavior of the K^+-Na^+ symport will be significantly altered in cell fragments. Figure 5*a* and *b* shows the membrane currents induced in a number of cells, by the addition of K^+ to a background solution of Na^+, and vice-versa. Results such as these demonstrate that the kinetics of this symport in cell fragments will resemble that in intact cells for the following reasons:

i) The transport operates under the same conditions (i.e., low $[K^+]_o$), and relatively large current changes are observed from exposure to very small (micromolar) concentrations of K^+.

ii) K^+ currents are observed only in the presence of Na^+, and similarly Na^+ currents require the

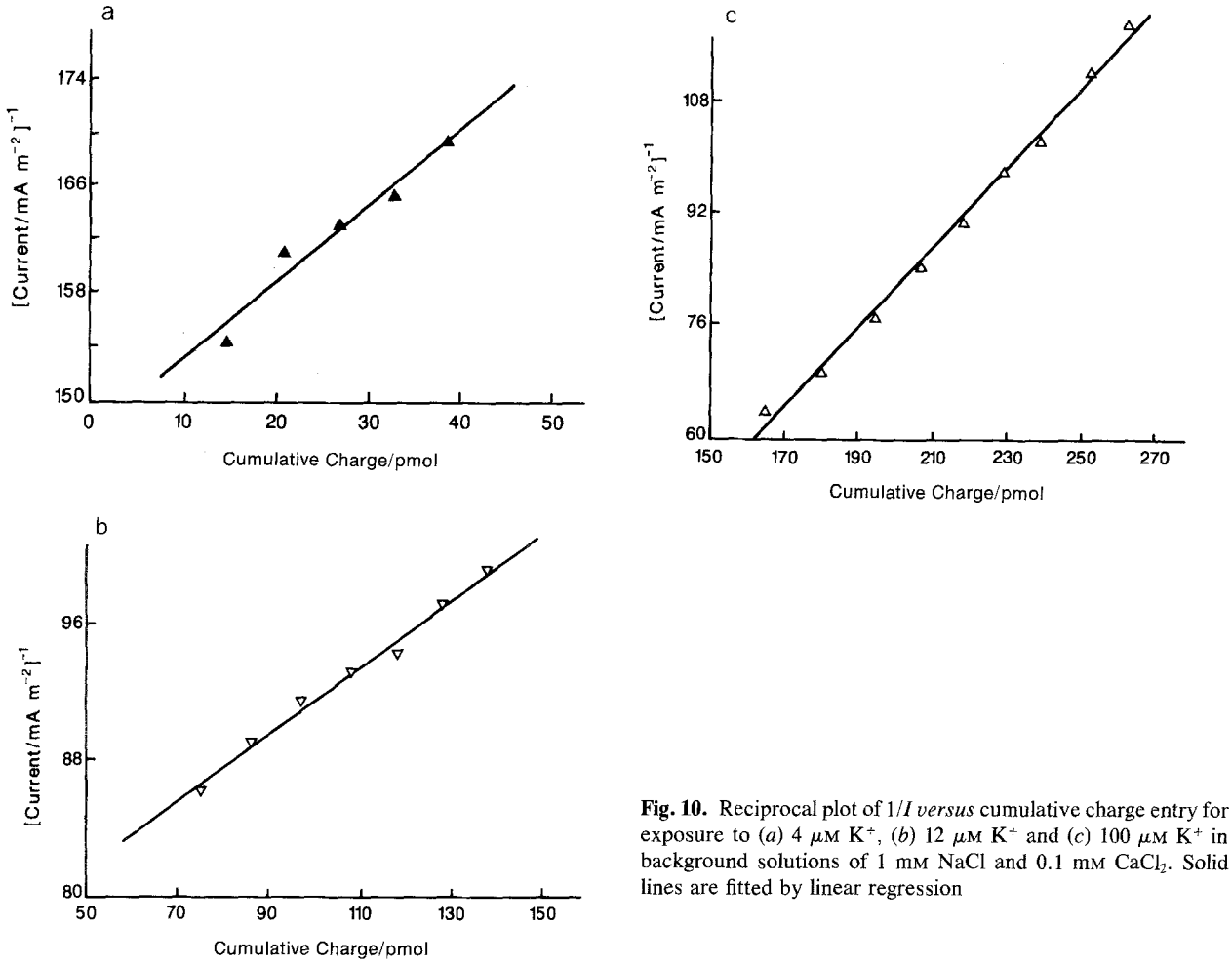

Fig. 10. Reciprocal plot of $1/I$ *versus* cumulative charge entry for exposure to (*a*) 4 μM K^+, (*b*) 12 μM K^+ and (*c*) 100 μM K^+ in background solutions of 1 mM NaCl and 0.1 mM $CaCl_2$. Solid lines are fitted by linear regression

presence of K^+, consistent with the observations by Smith and Walker (1989).

iii) The magnitude of the currents observed in cell fragments (Fig. 5*a* and *b*) are of similar magnitude to those observed in intact cells in this study, and also by Smith and Walker (1989).

iv) Similar onset times for the currents (of the order of seconds) were observed in both cell fragments and intact cells.

Difference *I-V* Curves

It was noted in the results that the *dI-V* curves of Fig. 6 apparently contradict the prediction by Blatt (1986) that difference *I-V* curves should always lie negative to the voltage axis. This, as Blatt points out, requires that changes in the experimental conditions only affect the transport protein under investigation and also that there is no current through the transport system at any voltage under the control conditions. It seems reasonable, however, to think that in *Chara* the more important problem is that the *I-V* curves are dominated so much by large rectifier currents at low potentials that the small K^+-Na^+ currents become "swamped," making it very difficult to distinguish them accurately from the large rectifier currents. A similar problem exists in the region of hyperpolarizing potentials, where the large outflow of Cl^- dominates the *I-V* curves. Thus difference *I-V* curves are more accurate over a limited voltage range where they are unaffected by these large currents. This is consistent with the restriction imposed by Blatt et al. (1987), that *Neurospora* difference *I-V* curves at potentials negative to about -125 mV should contain negligible subtraction error.

Modeling the K^+-Na^+ Symport

An important feature of the symport kinetics which emerges from the results of Figs. 7-9, is that the kinetic parameters K_m and V_{max} for both K^+ and Na^+ were found to vary with membrane potential, suggesting that the transport is limited at low membrane potential. This finding forms the basis for considering possible kinetic models for the K^+-Na^+ symport, by analogy to the behavior of the K^+-H^+ in *Neurospora* (Blatt et al., 1987).

A method commonly used for interpreting the results of membrane transport experiments has been to model the system as a series of reaction steps which form a closed cycle (e.g., Eilam & Stein, 1974; Hansen et al., 1981; Sanders et al., 1984; Blatt, 1986; Fisahn, Hansen & Grandmann, 1986; Sanders, 1986; Blatt et al., 1987; Gradmann, Klieber & Hansen, 1987). In order to keep the models as simple and general as possible, no explicit physical assumptions about the transport are made, other than to suppose that the ligands traverse the membrane by reacting with a species of protein molecule which is confined to the cell membrane.

For the case of cotransport involving two ions, there is a minimum of six reaction steps in a complete cyclic reaction scheme (e.g., Hansen et al., 1981; Sanders et al., 1984; Blatt et al., 1987). For the case of this K^+-Na^+ symport, the models of Blatt et al. (1987) may be adapted to this system by simply replacing H^+ with Na^+.

Alternative Models

The behavior of these types of models has been described in considerable detail (e.g., Hansen et al., 1981; Sanders et al., 1984); they are found to be versatile in their ability to describe a wide range of experimental results. The models themselves, however, are somewhat restrictive in that they require the "simultaneous" transport of both ions together in a single membrane transit step. For this reason, an investigation of alternative reaction schemes was initiated as part of this study.

In the additional model type considered, the K^+ and Na^+ ions are allowed to transit the membrane in two distinct reaction steps. A scheme such as this has been described as a "consecutive" transport mechanism by Jaunch and Läuger (1986), as opposed to the "simultaneous" models described previously. Following the arguments of Blatt et al. (1987), it is possible to represent these models in a reduced form under conditions where little information is known about intracellular steps. The consecutive models are illustrated in Fig. 11, where to each reaction step, reaction constants k_{ij} and k_{ji} have been assigned for the forward and reverse transitions between states N_i and N_j, respectively, consistently with previous conventions (Blatt, 1986; Sanders et al. 1984; Blatt et al., 1987). The models illustrated represent the following cases: the transport protein itself carries no net charge in any of the reaction steps, so that voltage-dependent steps occur only as either K^+ or Na^+ cross the membrane (model I). Model II represents the situation when part of the transport protein carries a single negative charge, so that a voltage-dependent step will occur as this charge traverses the membrane upon the protein returning to its original configuration; in this case, the first voltage-dependent step may occur as either the first or the second ion traverses the membrane, as represented by models II(a) and II(b). The third model allows for a single voltage-dependent step as the protein, which carries a double negative charge, returns to its initial state.

For each model it is possible (under limiting experimental conditions) to find expressions for K_m and V_{max} as functions of the reaction constants, including explicitly the dependence of these parameters on membrane potential. Again, the simultaneous models of Blatt et al. (1987) can be adapted to the K^+-Na^+ symport by replacing H^+ with Na^+ in each of these expressions.

The corresponding expressions for the consecutive models were derived specifically for this study. The results are summarized in the Table. Expressions such as those in the Table show that the behavior of these models depends largely on the relative magnitudes of individual reaction constants in the overall transport cycle. For each model, various properties of K_m and V_{max} are possible, depending on the relative sizes of the terms which determine these parameters, and different models may be able to yield similar behavior for either or both of K_m and V_{max}. In order to determine which models are feasible for a particular transport system, it is necessary to find which models (if any) can describe the observed kinetic data without requiring inconsistencies in the sizes of any reaction constants.

Identifying a Consistent Model for the K^+-Na^+ Symport

In examining the results of Figs. 8 and 9, it is necessary to point out that K^+ is treated as the substrate ion in experiments for which $[Na^+]_o$ was fixed, and similarly Na^+ becomes the primary substrate when $[K^+]_o$ remains constant. The result that K_m and V_{max} for Na^+ simultaneously increase as the membrane potential becomes more negative can be shown to be consistent with all but one of the simultaneous

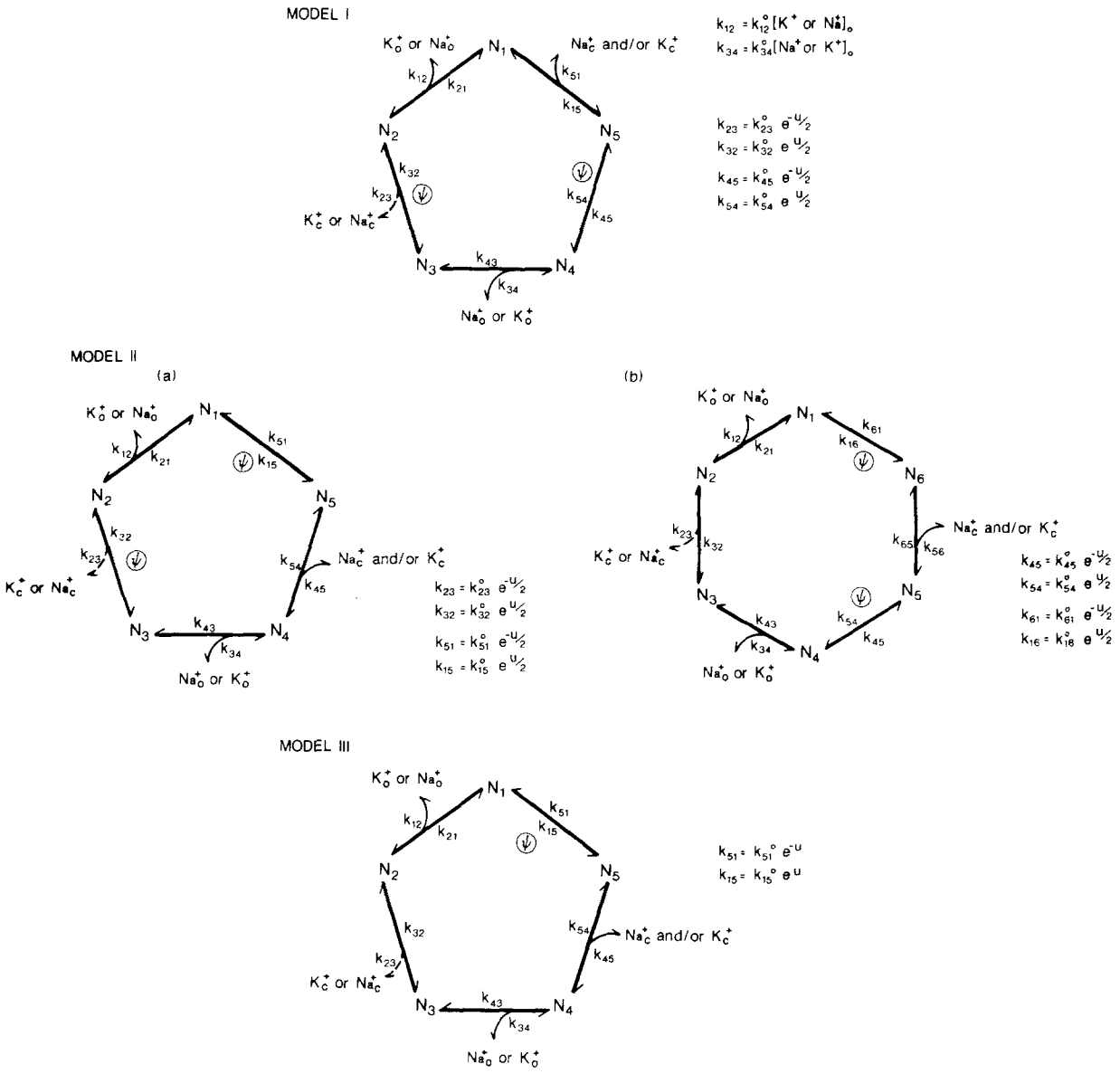

Fig. 11. Consecutive models for cotransport of K^+ and Na^+ (reduced forms only). The first ion is transported across the membrane between states N_2 and N_3. The second translocation step occurs between states N_4 and N_5. K^+ and Na^+ are transported into the cell on moving consecutively through states N_1 to N_5 in each model. Dashed lines represent possible translocation and subsequent release into the cytoplasm of the first-bound ion. Alternatively, both ions may be released together following translocation of the second ion across the membrane. Voltage-dependent steps are indicated by Ψ

models. Treating Na^+ as the substrate ion, only a model in which the protein carries one negative charge and Na^+ binds after K^+ cannot accommodate the observed behavior of K_m and V_{max}. The Table for the consecutive models, however, shows that only one of these is consistent with these results, namely Model III(L), where Na^+ binds after K^+. (All other consecutive models appear to require K_m to decrease as membrane potential becomes more negative.)

The second observation that K_m for K^+ decreases while V_{max} increases with increasing negative membrane potential (Fig. 8) seems to eliminate all but one of the possible simultaneous models, namely, the case where the protein carries a double negative charge and K^+ binds before Na^+. These same results, however, are consistent with three of the consecutive models, one of which is again the case where the protein carries two negative charges and K^+ binds before Na^+. Hence these last two models described, one simultaneous and one consecutive, are the only two models that may be selected on the basis of being consistent with all of the experimental results.

Table. Summary list of conditions which cause the specified changes ($\uparrow$ or $\downarrow$) of K_m and V_{max} for substrate S^+, as membrane potential is varied under conditions for saturating driver ion (D^+)[a]

Model	Binding order	K_m	$V_{max}/(-)2FN$
I(F)	S^+, D^+	$\dfrac{k_{15}k_{23}^o k_{54}^o + k_{21}k_{15}k_{54}^o e^{u/2} + k_{21}k_{45}^o e^{-u/2}(k_{15}+k_{51}) + k_{23}^o k_{45}^o e^{-u}(k_{15}+k_{51})}{k_{12}^o[k_{23}^o k_{54}^o + k_{23}^o k_{45}^o e^{-u} + e^{-u/2}(k_{45}^o + k_{23}^o)k_{51}]}$	$\dfrac{k_{51}k_{23}^o k_{45}^o e^{-u}}{k_{23}^o k_{54}^o + k_{45}^o k_{23}^o e^{-u} + e^{-u/2}(k_{45}^o + k_{23}^o)k_{51}}$
	$\uparrow$:	NC	k_{54}^o or $k_{51} \geq k_{45}^o$, or $k_{51} \geq k_{23}^o$
	$\downarrow$:	$k_{54}^o \gg k_{45}^o$, $k_{21}^o \gg k_{23}^o$	NC
I(L)	D^+, S^+	$\dfrac{k_{45}^o k_{32}^o k_{51} + k_{54}^o k_{23}^o k_{43} + k_{43}k_{54}^o k_{32}^o e^u + k_{51}k_{45}^o k_{23}^o e^{-u} + e^{-u/2}(k_{32}^o + k_{23}^o)k_{51}k_{43}}{k_{34}^o[k_{23}^o k_{54}^o + k_{45}^o k_{23}^o e^{-u} + e^{-u/2}(k_{23}^o + k_{45}^o)k_{51}]}$	$\dfrac{k_{51}k_{23}^o k_{45}^o e^{-u}}{k_{23}^o k_{54}^o + k_{45}^o k_{23}^o e^{-u} + e^{-u/2}(k_{45}^o + k_{23}^o)k_{51}}$
	$\uparrow$:	NC	k_{51} or $k_{54}^o \geq k_{45}^o$, or $k_{51} \geq k_{23}^o$
	$\downarrow$:	$k_{32}^o \gg k_{23}^o$, $k_{54}^o \gg k_{51}$	NC
IIa(F)	S^+, D^+	$\dfrac{k_{23}^o k_{15}^o(k_{45}+k_{54}) + e^{u/2}(k_{45}+k_{54}) + k_{21}k_{45}k_{51}^o e^{-u/2} + k_{45}k_{23}^o k_{51}^o e^{-u}}{k_{12}^o[e^{-u/2}(k_{45}k_{23}^o + k_{45}k_{51}^o + k_{54}k_{23}^o) + k_{23}^o k_{51}^o e^{-u}]}$	$\dfrac{k_{45}k_{23}^o k_{51}^o}{k_{23}^o k_{51}^o + e^{u/2}(k_{45}k_{23}^o + k_{45}k_{51}^o + k_{54}k_{23}^o)}$
	$\uparrow$:	NC	k_{54} or $k_{45} \geq k_{51}^o$, or $k_{45} \geq k_{23}^o$
	$\downarrow$:	$k_{15}^o \gg k_{51}^o$	NC
IIa(L)	D^+, S^+	$\dfrac{k_{32}^o k_{51}^o(k_{43}+k_{45}) + k_{43}k_{54}k_{32}^o e^{u/2} + k_{43}k_{54}k_{23}^o e^{-u/2} + e^{-u}(k_{43}+k_{45})k_{23}k_{51}^o}{k_{34}^o[k_{23}^o k_{51}^o + e^{-u/2}(k_{45}k_{23}^o + k_{45}k_{51}^o + k_{54}k_{23}^o)]}$	$\dfrac{k_{45}k_{23}^o k_{51}^o}{k_{23}^o k_{51}^o + e^{u/2}(k_{45}k_{23}^o + k_{45}k_{51}^o + k_{54}k_{23}^o)}$
	$\uparrow$:	NC	k_{54} or $k_{45} \geq k_{51}^o$, or $k_{45} \geq k_{23}^o$
	$\downarrow$:	$k_{32}^o \gg k_{23}^o$	NC
IIb(F)	S^+, D^+	$\dfrac{k_{16}^o k_{45}^o(k_{56}+k_{65})(k_{23}+k_{21}) + e^u(k_{23}+k_{21})k_{65}k_{54}^o k_{16}^o + e^{-u}(k_{21}+k_{23})k_{56}k_{61}^o k_{45}^o}{k_{12}^o[k_{23}k_{54}^o k_{61}^o + e^{u/2}k_{65}k_{23}k_{54}^o + e^{-u/2}(k_{56}k_{45}^o + k_{56}k_{61}^o + k_{65}k_{45}^o)k_{23} + e^{-u}(k_{56}+k_{23})k_{61}^o k_{45}^o]}$	$\dfrac{k_{23}k_{56}k_{45}^o k_{61}^o}{k_{45}^o k_{61}^o(k_{23}+k_{56}) + k_{23}[e^{3u/2}k_{65}k_{54}^o + e^u k_{54}^o k_{61}^o + e^{u/2}(k_{56}k_{45}^o + k_{56}k_{61}^o + k_{65}k_{45}^o)]}$
	$\uparrow$:	NC	$k_{54}^o \gg k_{45}^o$ or $k_{65} \gg k_{61}^o$
	$\downarrow$:	$k_{45}^o \gg k_{54}^o$ and $k_{16}^o \gg k_{61}^o$	NC
IIb(L)	S^+, D^+	$\dfrac{(k_{23}+k_{32})[k_{43}k_{54}^o k_{61}^o + k_{43}k_{65}k_{54}^o e^{u/2} + k_{43}k_{56}k_{61}^o e^{-u/2} + k_{56}k_{45}^o k_{61}^o e^{-u}]}{k_{34}^o[k_{23}k_{54}^o k_{61}^o + k_{23}k_{65}k_{54}^o e^{u/2} + e^{-u/2}(k_{56}k_{45}^o + k_{56}k_{61}^o + k_{65}k_{45}^o)k_{23} + e^{-u}(k_{23}+k_{56})k_{45}^o k_{61}^o]}$	$\dfrac{k_{23}k_{56}k_{45}^o k_{61}^o}{k_{45}^o k_{61}^o(k_{23}+k_{56}) + k_{23}[e^{3u/2}k_{65}k_{54}^o + e^u k_{54}^o k_{61}^o + e^{u/2}(k_{56}k_{45}^o + k_{56}k_{61}^o + k_{65}k_{45}^o)]}$
	$\uparrow$:	NC	$k_{54}^o \gg k_{45}^o$ or $k_{65} \gg k_{61}^o$
	$\downarrow$:	NC	NC

Table continued next page

Table. *Continued*

Model	Binding order	K_m	$V_{max}/(-)2FN$
III(F)	S^+, D^+	$\frac{k^o_{15}e^{u}(k_{23}+k_{21})(k_{54}+k_{45}) + k_{45}k^o_{51}e^{-u}(k_{23}+k_{21})}{k^o_{12}[k_{23}(k_{54}+k_{45}) + k^o_{51}e^{-u}(k_{23}+k_{45})]}$	$\frac{k_{23}k_{45}k^o_{51}e^{-u}}{k_{23}(k_{54}+k_{45}) + k^o_{51}e^{-u}(k_{23}+k_{45})}$
	↑:	NC	$k_{54} \gg k^o_{51}$
	↓:	$k^o_{15} \gg k^o_{51}$ or $k_{54} \gg k_{45}$	NC
III(L)	D^+, S^+	$\frac{k^o_{51}e^{-u}(k_{23}+k_{32})(k_{45}+k_{43}) + k_{54}k_{43}(k_{23}+k_{32})}{k^o_{34}[k^o_{51}e^{-u}(k_{45}+k_{23}) + k_{23}(k_{45}+k_{54})]}$	$\frac{k_{23}k_{45}k^o_{51}e^{-u}}{k_{23}(k_{54}+k_{45}) + k^o_{51}e^{-u}(k_{23}+k_{45})}$
	↑:	$k_{54} \gg k_{45}$ or k^o_{51}, $k^o_{51}k_{43}$	$k_{54} \gg k^o_{51}$
	↓:	NC	NC

[a] Conditions were derived from the steady-state rate equations formed from the consecutive models of Fig. 11. (NC = no conditions which can satisfy the required behavior.)

Implications of the Models

Although these two models for the K^+-Na^+ symport are based on different reaction schemes, they have several features in common. This is not a complete surprise, since the models differ only by the inclusion of an additional single ($[K^+]_o$-, $[Na^+]_o$- and voltage-independent) reaction step in the consecutive model. The addition of such a step should not have any qualitative effect on the behavior of a cotransport system (Hansen et al., 1981; Sanders et al., 1984).

In both models the transport is limited at low membrane potentials by the forward voltage-dependent reaction constant. Both models require that the protein has a double negative charge when unloaded, and that K^+ binds before Na^+ in each case. The significance of this binding order is that K^+ binding occurs adjacent to the voltage-dependent step in both models. This appears to be a concomitant of the decrease in K_m for K^+ as membrane potential becomes more negative, so that binding of K^+ to the protein can occur rapidly following charge transit. The fact that the models selected predict that a double negative charge is carried across the membrane by the unloaded protein returning to its original configuration implies that there is actual movement of some part of this protein within the membrane. In this sense it is possible to view this transport protein as a true "carrier" of electric charge.

Conclusions

1. Although voltage-clamp techniques using external electrodes were used to provide a quick and relatively simple method for determining membrane currents due to K^+-Na^+ symport in intact cells, cytoplasm-enriched fragments were found to be a better system for estimation of kinetic parameters, since they give rise to currents that do not fall off rapidly with time.

2. Intact-cell measurements gave rise to a rapid current turnoff. Our explanation for this effect is that it is caused by increasing $[Na^+]$ in the cytoplasm. A general model for cotransport is used to show that this effect should occur and should be greater for high $[K^+]_o$. This is consistent with the experimental results.

3. K_m for K^+ was found to decrease as membrane potential became more negative, while K_m for Na^+ was observed to increase. Kinetic modelling suggests that the membrane charge-transit process is the limiting step in the overall transport scheme at low membrane potentials.

The experimental results are consistent with two possible cotransport models, one of which is of "consecutive" type. Both models identify the carrier protein as having a double negative charge in its unloaded form, and both predict that the extracellular binding is ordered as K^+ followed by Na^+.

While several variations of the consecutive model are possible, this study has shown that at least some of these are useful in complementing the existing cotransport models.

This work formed part of S.R. McCulloch's 1988 Honours project in the School of Biological Sciences, University of Sydney, to whom we are grateful for support. We also thank the Australian Research Grants Scheme for support, and Dr. F.A. Smith for a critical reading of the manuscript.

References

Bakker, E.P., Harold, F.M. 1980. Energy coupling to potassium transport in *Streptococcus faecalis*. *J. Biol. Chem.* **255**:433–440

Barry, P.H., Diamond, J.M. 1984. Effects of unstirred layers on the membrane phenomena. *Physiol. Rev.* **63**:763–872

Beilby, M.J., 1986*a*. Potassium channels and different states of *Chara* plasmalemma. *J. Membrane Biol.* **89**:241–249

Beilby, M.J., 1986*b*. Factors controlling the K^+ conductance in *Chara*. *J. Membrane Biol.* **93**:187–193

Beilby, M.J., Beilby, B.N. 1983. Potential dependence of the admittance of *Chara* plasmalemma. *J. Membrane Biol.* **74**:229–245

Beilby, M.J., Blatt, M.R. 1986. Simultaneous measurements of cytoplasmic K^+ concentration and the plasma membrane electrical parameters in single membrane samples of *Chara corallina*. *Plant Physiol.* **82**:417–422

Beilby, M.J., Shepherd, V.A. 1989. Cytoplasm-enriched fragments of *Chara:* structure and electrophysiology. *Protoplasma* **148**:150–163

Beilby, M.J., Walker, N.A. 1981. Chloride transport in *Chara:* I. Kinetics and current voltage curves for a probable proton symport. *J. Exp. Bot.* **32**:43–54

Blatt, M.R. 1986. Interpretation of steady-state current-voltage curves: Consequences and implications of current subtraction in transport studies. *J. Membrane Biol.* **92**:91–110

Blatt, M.R., Rodriguez-Navarro, A., Slayman, C.L. 1987. Potassium-proton symport in *Neurospora:* Kinetic control by pH and membrane potential. *J. Membrane Biol.* **98**:169–189

Bostrom, T.E., Walker, N.A. 1975. Intracellular transport in plants. I. The rate of transport of chloride and electrical resistance. *J. Exp. Bot.* **26**:767–782

Coleman, H.A. 1986. Chloride currents in *Chara*—A patch-clamp study. *J. Membrane Biol.* **93**:55–61

Cornish-Bowden, A. 1979. Fundamentals of Enzyme Kinetics. Butterworths, London—Boston

Coster, H.G.L. 1965. A quantitative analysis of the voltage-current relationships of fixed charge membranes and the associated property of "punch-through." *Biophys. J.* **5**:669–686

Coster, H.G.L., Hope, A.B. 1968. Ionic relations of cells of *Chara australis*. *Aust. J. Biol. Sci.* **21**:243–254

Eilam, Y., Stein, W.D. 1974. Kinetic studies of transport across red blood cell membranes. *In:* Methods in Membrane Biology. Vol. 2, pp. 283–354. Edward D. Korn, editor. Plenum, New York

Felle, H. 1981. A study of the current-voltage relationships of the electrogenic active and passive membrane elements in *Riccia fluitans*. *Biochim. Biophys. Acta* **646**:151–160

Fisahn, J., Hansen, U-P., Gradmann, D. 1986. Determination of charge, stoichiometry and reaction constants from *I-V* curve studies on a K^+ transporter in *Nitella*. *J. Membrane Biol.* **94**:245–252

Gradmann, D., Klieber, H.-G., Hansen, U.-P. 1987. Reaction kinetic parameters for ion transport from steady-state current-voltage curves. *Biophys. J.* **51**:569–585

Hansen, U.-P., Gradmann, D., Sanders, D., Slayman, C.L. 1981. Interpretation of current-voltage relationships for "active" ion transport systems: I. Steady-state reaction-kinetic analysis of class-I mechanisms. *J. Membrane Biol.* **63**:165–190

Hill, R., Whittingham, C.P. 1957. Photosynthesis. Methuen, London

Hirono, C., Mitsui, T. 1981. Time course of activation in plasmalemma of *Nitella axilliformis*. *In:* Nerve Membrane. G. Matsumoto and M. Kotani, editors. pp. 135–149. University of Tokyo Press, Tokyo

Hope, A.B., Walker, N.A. 1961. Ionic relations of cells of *Chara australis* R. Br: IV. Membrane potential differences and resistances. *Aust. J. Biol. Sci.* **14**:26–44

Jaunch, P., Läuger, P. 1986. Electrogenic properties of the sodium-alanine cotransporter in pancreatic acinar cells: II. Comparison with transport models. *J. Membrane Biol.* **94**:117–127

Keifer, D.W., Lucas, W.J. 1982. Potassium channels in *Chara corallina*. Control and interaction with the electrogenic H^+ pump. *Plant Physiol.* **69**:781–788

Kitasato, H. 1973. K permeability of *Nitella clavata* in the depolarised state. *J. Gen. Physiol.* **62**:535–549

Peebles, M.J., Mercer, F.V., Chambers, T.C. 1964. Studies on the comparative physiology of *Chara australis:* I. Growth pattern and gross cytology of the internodal cell. *Aust. J. Biol. Sci.* **17**:49–61

Press, W.H., Flannery, B.P., Teukolsky, S.A., Vetterling, W.T. 1987. Numerical Recipes. Cambridge University Press, Cambridge

Rodriguez-Navarro, A. Blatt, M.R., Slayman, C.L. 1986. A potassium-proton symport in *Neurospora crassa*. *J. Gen. Physiol.* **87**:649–674

Sakano, K., Tazawa, M. 1984. Intracellular distribution of free amino acids between the vacuolar and extravacuolar compartments in internodal cells of *Chara australis*. *Plant Cell Physiol.* **25**:1477–1486

Sanders, D. 1980. Control of Cl^- influx in *Chara* by cytoplasmic Cl^- concentration. *J. Membrane Biol.* **52**:51–60

Sanders, D. 1986. Generalized kinetic analysis of ion-driven cotransport systems: II. Random ligand binding as a simple explanation for non-Michaelian kinetics. *J. Membrane Biol.* **90**:67–87

Sanders, D., Hansen, U.-P., Gradmann, D., Slayman, C.L. 1984. Generalized kinetic analysis of ion-driven cotransport systems: A unified interpretation of selective ionic effects on Michaelis parameters. *J. Membrane Biol.***77**:123–152

Smith, F.A., Walker, N.A. 1989. Transport of potassium in *Chara australis:* I. A symport with sodium. *J. Membrane Biol.* **108**:125–137

Smith, J.R., Smith, F.A., Walker, N.A. 1987. Potassium transport across the membranes of *Chara:* I. The relationship between radioactive tracer influx and electrical conductance. *J. Exp. Bot.* **38**:731–751

Smith, P.T. 1984. Electrical evidence from perfused and intact cells for voltage-dependent K^+ channels in the plasmalemma of *Chara australis*. *Aust. J. Plant Physiol.* **11**:303–318

Tazawa, M., Kishimoto, U. Kikuyama, M. 1974. Potassium, sodium and chlorine in the protoplasm of characeae. *Plant Cell Physiol.* **15**:103–110

Tyerman, S.D., Findlay, G.P., Paterson, G.J. 1986*a*. Inward membrane current in *Chara inflata:* I. A voltage- and time-dependent Cl^- component. *J. Membrane Biol.* **89**:139–152

Tyerman, S.D., Findlay, G.P., Paterson, G.J. 1986*b*. Inward membrane current in *Chara inflata:* II. Effects of pH, Cl^--channel blockers and NH_4^+, and significance for the hyperpolarized state. *J. Membrane Biol.* **89**:153–161

Walker, N.A. 1980. The transport systems of charophyte and chlorophyte giant algae and their integration into modes of behaviour. *In:* Plant Membrane Transport: Current Conceptual Issues. R.M. Spanswick, W.J. Lucas and J. Dainty, editors. pp. 287–304. Elsevier/North Holland Biomedical, Amsterdam

Walker, N.A., Beilby, M.J., Smith, F.A. 1979. Amine uniport at the plasmalemma of charophyte cells: I. Current-voltage curves, saturation kinetics, and effects of unstirred layers. *J. Membrane Biol.* **49**:21–55

Received 7 July 1989; revised 15 November 1989